# Photogeneration and Decay of Charge Carriers in Hybrid Bulk Heterojunctions of ZnO Nanoparticles and Conjugated Polymers†

**Pieter A. C. Quist,‡ Waldo J. E. Beek,§ Martijn M. Wienk,§ René A. J. Janssen,§ Tom J. Savenije,*,‡ and Laurens D. A. Siebbeles‡**

*Opto-Electronic Materials Section, DelftChemTech, Faculty of Applied Sciences, Delft University of Technology, Julianalaan 136, NL-2628 BL Delft, The Netherlands, and Molecular Materials and Nanosystems, Eindhoven University of Technology, P.O. Box 513, NL-5600 MB Eindhoven, The Netherlands*

*Received: September 27, 2005; In Final Form: December 20, 2005*

The photogeneration and decay of charge carriers in blend films of ZnO nanoparticles (diameter 5 nm) and poly[2-methoxy-5-(3′,7′-dimethyloctyloxy)-1,4-phenylenevinylene] (MDMO-PPV) or poly(3-hexylthiophene) (P3HT) were studied by means of microwave-photoconductance measurements. Excitation of the polymer in the visible spectrum was found to lead to a transient photoconductance due to dissociation of excitons at the interface between ZnO and the conjugated polymer. From the similar decay kinetics of the photoconductance and the effects of UV illumination, it is concluded that the measured photoconductance is due to electrons in ZnO. Increasing the weight fraction of ZnO in the blend films leads to a higher photoconductance. This is attributed to enhanced formation of mobile electrons by interfacial dissociation of excitons at clusters of ZnO nanoparticles rather than at individual nanoparticles. The dependence of the photoconductance on the weight fraction of ZnO is found to be different for ZnO:MDMO-PPV and ZnO:P3HT blends. This is most likely due to the presence of a smaller number of relatively large ZnO clusters in ZnO:P3HT blends and a shorter exciton diffusion length, as compared with ZnO:MDMO-PPV blends. After exposure of the blend films to UV light, a significant increase in the magnitude and the lifetime of the photoconductance is observed. This is explained in terms of the filling of electron traps in ZnO by UV exposure.

## Introduction

The high costs involved in the production of high purity crystalline silicon form a barrier to the large-scale application of solar cells based on this material. Therefore, the development of solar cells based on alternative materials currently attracts a great deal of attention.[1] A promising approach is the combination of a wide band gap semiconductor and an organic dye. In these systems, the dye absorbs solar light, leading to the formation of excitons. The excitons can undergo dissociation into free charge carriers at the interface with the electron-accepting semiconductor. Using this approach, a breakthrough in cell performance was achieved by Gratzel and Oregan,[2] who developed an anatase nanocrystalline $TiO_2$ electrode covered with a ruthenium dye. In combination with a liquid electrolyte containing an $I_3/I^-$ redox couple to regenerate the oxidized dye power, conversion efficiencies over 10% have been achieved.[2]

During the past decade, there has been a growing interest in the development of cheap hybrid organic/inorganic photovoltaic cells consisting of a wide band gap semiconductor and a conjugated polymer as sensitizer.[3−8] In these hybrid photovoltaic cells, the conjugated polymer absorbs light, leading to electron injection into the conduction band of the semiconductor. The hole is transported to a metal back contact via the conjugated polymer. Conjugated polymers have promising prospects for application in solar cells, including low cost, mechanical flexibility, and strong absorption in the visible, while their electronic properties can easily be tuned by chemical modifications.

Several studies on combinations of a conjugated polymer with anatase $TiO_2$ for photovoltaic applications have been carried out.[3−6,9,10] It has been found that excitons produced by photoexcitation of the polymer can diffuse over a distance on the order of 10 nm prior to (non)radiative decay. Hence, only those excitons that are produced within this distance from the interface between the polymer and the semiconductor can contribute to the photovoltaic effect. Since the penetration depth of solar light largely exceeds the exciton diffusion length, the efficiency of photovoltaic cells consisting of a simple bilayer of a polymer and a semiconductor is low.[3,10,11] A way to overcome this problem is to use bulk heterojunctions of a polymer and a nanostructured semiconductor. In such a blend, both materials are in intimate contact and excitons need to diffuse over a relatively short distance to reach the interface between the polymer and the semiconductor.

The AM1.5 conversion efficiencies achieved with photovoltaic cells based on a bulk heterojunction of nanocrystalline $TiO_2$ and a conjugated polymer were found to be below 0.5%.[7,12,13] The main problem is the incompatibility of both compounds to dissolve in a single spin-coating solvent, leading to the formation of relatively large domains consisting of either $TiO_2$ or the conjugated polymer. As shown by Beek et al.,[14] this problem can be overcome by using ZnO as the electron-accepting semiconductor instead of $TiO_2$. It was found to be possible to produce stable solutions of 5 nm sized ZnO nanoparticles and poly[2-methoxy-5-(3′,7′-dimethyloctyloxy)-1,4-phenylenevinylene] (MDMO-PPV) in chlorobenzene, which were used to

* Correspondence. E-mail: T.J.Savenije@tnw.tudelft.nl. Phone: +31 15 2786537. Fax: +31 15 2787421.

† The work of P. A. C. Quist and M. M. Wienk forms part of the research program of the Dutch Polymer Institute (DPI).

‡ Delft University of Technology.

§ Eindhoven University of Technology.

10.1021/jp055492m CCC: $33.50 
Published on Web 05/11/2006

produce hybrid cells with an energy conversion efficiency of 1.6% under AM1.5.[14,15] Studies of the effect of the content of ZnO in the photoactive layer have shown that the optimal weight fraction of ZnO is equal to $W_{ZnO} = 0.67$, corresponding to a volume fraction equal to 0.25.[14,15]

The present work aims to provide further insight into the factors that govern the efficiency of this new class of hybrid solar cell based on blends of a conjugated polymer and ZnO nanoparticles. Results are presented for blends of ZnO and either MDMO-PPV or regioregular poly(3-hexylthiophene) (P3HT). P3HT is of interest due to more favorable solar light absorption and a higher hole mobility as compared to MDMO-PPV. Prospects for application of ZnO:P3HT blends in solar cells are discussed. Recently, these blends have been characterized by measurements of transient absorption, fluorescence, and *I*/*V*-characteristics.[16] The present study focuses on optical absorption spectroscopy and the photoconducting properties obtained from electrodeless time-resolved microwave conductivity (TRMC) measurements. An important advantage of the TRMC technique is that the intrinsic AC photoconductance of the blend films can be measured without the necessity of applying electrodes to the sample. With the TRMC technique, the local motion of charge carriers in the oscillating microwave electric field is probed and consequently the conductance is not affected by the film thickness. The results provide insight into the effect of the blend composition on the efficiency of charge carrier formation and the kinetics of charge carrier decay. The knowledge obtained can be of use to give direction to the improvement of the performance of hybrid organic/inorganic solar cells.

It has been found earlier that the performance of hybrid solar cells based on a blend of ZnO and a conjugated polymer is strongly dependent on the weight fraction ZnO.[14,15] Therefore, in the present work, particular attention is paid to the effect of $W_{ZnO}$ on the efficiency of the photogeneration of charge carriers.

In addition, the effect of UV illumination prior to recording the photoconductance of ZnO:P3HT blend films on visible excitation was studied. UV illumination was found to lead to a significant increase of both the magnitude and the lifetime of the photoconductance due to filling of traps by charges that are generated by UV excitation of ZnO. The latter result provides an explanation for the disappearance of the photovoltaic effect of solar cells after UV illumination.[15]

## Experimental Section

**Sample Preparation.** Poly[2-methoxy-5-(3′,7′-dimethyloctyloxy)-1,4-phenylenevinylene] (MDMO-PPV), synthesized via the Gilch route,[17] was used as received. Regioregular poly(3-hexylthiophene) (P3HT), obtained from Rieke, was purified after reduction with hydrazine by precipitation in methanol and subsequent Soxhlet extraction in dichloromethane ($CH_2Cl_2$) and chloroform ($CHCl_3$), yielding a polymer with $M_W = 1.7 \times 10^5$ g/mol. ZnO nanoparticles with a diameter of 5 nm were prepared as described by Beek et al.[18] and have been characterized with transmission electron microscopy (TEM) as described in refs 14 and 18.

The ZnO:MDMO-PPV blend films were prepared from chlorobenzene similar to the studies on photovoltaic devices of this material.[14,15] Unfortunately, using chlorobenzene as solvent, stable solutions of ZnO and P3HT cannot be obtained. However, photovoltaic cells based on ZnO:P3HT blend films have been prepared using chloroform as a solvent.[16] To facilitate comparison of the data from the current work with those in ref 16, the ZnO:P3HT blend films were prepared from chloroform. Chlorobenzene solutions of MDMO-PPV and ZnO nanoparticles were prepared by dissolving typically 3 mg of MDMO-PPV in 0.5 mL to which an appropriate volume of the ZnO nanoparticle stock solution was added. To improve the dispersion of the ZnO nanoparticles in the polymer solution, approximately 2 vol % methanol was added. Blend films of ZnO:MDMO-PPV were spin-coated (speed 1500 rpm) onto 1 mm thick, $12 \times 25$ mm$^2$ quartz substrates (ESCO products). Samples with P3HT were prepared from chloroform solution with a higher polymer concentration of 6 mg/mL. This resulted in film thicknesses of ca. 100 nm for samples with MDMO-PPV and ca. 150 nm for samples with P3HT. The maximum attainable weight fraction of ZnO was found to be 0.83, due to the instability of spin-coating solutions with higher ZnO content. The blend films are denoted as MDMO-PPV$_x$ or P3HT$_x$, with $x$ being the weight fraction of ZnO.

A Perkin-Elmer Lambda 900 UV/Vis/NIR spectrophotometer equipped with an integrating sphere (Lab sphere) was used to determine the absorption (OD) and attenuation ($F_A$) spectra from the fraction of incident light reflected and transmitted by the sample.[11]

**Flash-Photolysis Time-Resolved Microwave Conductivity (FP-TRMC).** Time-resolved measurements of the microwave conductivity due to charge carriers that are generated by pulsed photoexcitation of the sample were carried out using the experimental facility described extensively in ref 11. Laser pulses with a 3 ns full width at half-maximum (fwhm) continuously tunable from 420 to 700 nm were generated by pumping an optical parametric oscillator (OPO) with a Nd:YAG laser (Infinity 15-30, Coherent). The intensity of the laser beam could be attenuated using a series of metal-coated neutral-density filters (Melles Griot) in tandem, yielding a total number of incident photons per unit area per pulse ($I_0$) ranging from $10^{12}$ to $10^{16}$ photons/cm$^2$.[11]

Immediately after preparation, the samples were mounted in an X-band microwave cavity for photoconductance measurements. To avoid any contribution to the photoconductance by electrons photoejected from the sample, the microwave cavity was filled with an $CO_2/SF_6$ mixture so that the photoejected electrons are captured to form low mobility molecular anions.[19]

The photoinduced change in the conductance, $\Delta G(t)$, of the sample was obtained from the relative change in the microwave power (frequency 8.5 GHz) reflected by the cavity ($\Delta P(t)/P$) using nanosecond time-response microwave circuitry and detection equipment described previously.[11] The relation between these quantities is given by

$$\Delta G(t) = -\frac{\Delta P(t)/P}{K} \qquad (1)$$

where $K = 40 \times 10^3 \Omega$ is the known sensitivity factor of the cavity containing the sample. The amplitude of the microwave electric field in the cavity is equal to ca. 100 V/cm. The photoconductance $\Delta G(t)$ is proportional to the product of the number of charge carrier pairs present at time $t$ and the sum of the mobility of a positive and a negative charge carrier, $\Sigma\mu$. In the experiments, the photoconductance $\Delta G(t)$ initially increases due to generation of charge carriers during the laser pulse and subsequently decreases due to recombination and/or trapping of charges. The rise time of the photoconductance is determined by the 18 ns time response of the microwave cavity cell. The product $\eta\Sigma\mu$, with $\eta$ defined as the ratio of the number of charge carrier pairs at the maximum of the $\Delta G(t)$ transient and the total number of *incident* photons can be calculated using the relation

$$\eta\Sigma\mu = \frac{\Delta G_{max}}{\beta e I_0} \quad (2)$$

where $\beta = 2.1$ corresponds to the ratio of the rectangular dimensions of the waveguide used and $e$ is the elementary charge. To compare samples with different optical attenuation, the value of $\eta\Sigma\mu$ is divided by $F_A$. The ratio $\eta/F_A$ is equal to the number of charge carrier pairs per *absorbed* photon and can be considered as the equivalent of the internal quantum efficiency of a photovoltaic cell.

## Results & Discussion

**Optical Properties.** Figure 1 shows the optical absorption spectra of spin-coated films of the pure compounds, i.e., ZnO nanoparticles, MDMO-PPV, and regioregular P3HT and spectra of blend layers with $W_{ZnO} = 0.67$. The spectra are normalized to their maxima to facilitate comparison.

The film of ZnO nanoparticles absorbs in the UV with the absorption onset at 370 nm. Quantum confinement of electrons in the ZnO nanoparticles[20] causes the absorption onset to appear at a shorter wavelength than for a macroscopic ZnO crystal (392 nm).[21,22] According to the results by Pesika et al.,[21,22] an absorption onset at 370 nm implies that the ZnO nanoparticles have a diameter of 5.4 nm, which is close to the value of 5 nm determined by TEM.[14] From TEM measurements on ZnO:MDMO-PPV blends by Beek et al.,[18] it is apparent that the ZnO nanoparticles form an aggregated three-dimensional network of ZnO clusters. Apparently, aggregation does not significantly affect the optical absorption of the ZnO nanoparticles.

The polymer films mainly absorb in the visible with a maximum near 500 nm. Due to the different absorption spectra of ZnO and the polymers, the latter can be selectively photoexcited in the visible part of the spectrum. Within the visible range, the spectra of a pure MDMO-PPV layer and the MDMO-$PPV_{0.67}$ blend layer are similar. In contrast, the spectra of the pure P3HT layer and the $P3HT_{0.67}$ blend layer differ by the presence of a shoulder at the red side of the spectrum of pure P3HT. This shoulder has been attributed to the lamellar organization of polythiophene chains.[23] The nanoparticles most likely distort this organization, resulting in the disappearance of the shoulder.

**Processes Occurring after Photoexcitation.** The processes that may occur upon photoexcitation of the polymer in a blend with ZnO include the following:

$$P \xrightarrow{h\nu} P^* \quad (A)$$

$$P^* \rightarrow P \quad (B)$$

$$P^* + (ZnO)K \rightarrow P^+ + [(ZnO)K]^- \quad (C)$$

$$P^* + [(ZnO)K]_n \rightarrow P^+ + [(ZnO)K]_n^- \quad (D)$$

$$P^+ + [(ZnO)K]^- \rightarrow P + [(ZnO)K] \quad (E)$$

$$P^+ + [(ZnO)K]_n^- \rightarrow P + [(ZnO)K]_n \quad (F)$$

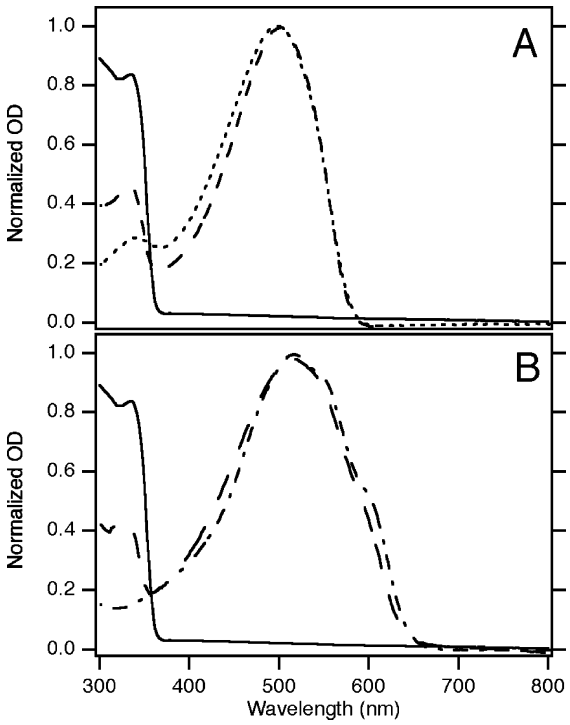


**Figure 1.** (A) Normalized optical density (OD) spectra of ZnO (full line), MDMO-PPV (dotted line), and the MDMO-$PPV_{0.67}$ blend film (dashed line). (B) Normalized optical density (OD) spectra of ZnO (full line), P3HT (dotted−dashed line), and the $P3HT_{0.67}$ blend film (long dashed line).

$$[(ZnO)K]_n^-(e_{free}) \rightarrow [(ZnO)K]_n^-(e_{trap}) \quad (G)$$

In the scheme above, an individual ZnO nanoparticle is denoted as (ZnO)K, while $[(ZnO)K]_n$ refers to a cluster of $n$ ZnO nanoparticles. Photoexcitation of the polymer results in the formation of excitons (A), which can decay back to the ground state by fluorescence or a nonradiative transition (B). During their lifetime, excitons may diffuse to an interface with an individual ZnO nanoparticle (C) or reach a cluster consisting of $n$ (>1) ZnO nanoparticles (D). At the interface with ZnO, excitons can dissociate into charge carriers, leading to electron injection into ZnO and the production of a hole in the polymer. Opposite charges can recombine with each other (E and F), while electrons in a ZnO cluster may also become trapped at a defect site (G).

**Photoconductance Transients.** Figure 2A shows the microwave conductance transients of pure MDMO-PPV and ZnO films and of the MDMO-$PPV_{0.67}$ blend film on photoexcitation at 510 nm. Clearly, a much larger and longer-lived signal is observed for the blend layer than for the films of the individual compounds. This is attributed to electron transfer from the polymer to the ZnO nanoparticles (processes C and D). The initial rise time of the TRMC signals largely exceeds the laser pulse duration (3 ns), due to the 18 ns time-response of the microwave cavity cell. After reaching a maximum at approximately 30 ns after the laser pulse, the signal decays as a result of trapping and/or recombination of the charge carriers. Note that the origin of the decay of the TRMC signal differs from the cause of the current decay in, e.g., time-of-flight measurements, which is due to collection of charges at the electrodes. Figure 2B compares the microwave conductance transients of the MDMO-$PPV_{0.67}$ and $P3HT_{0.67}$ blend films on photoexcitation at 510 and 480 nm, respectively.

Figure 3 shows the values of $\eta\Sigma\mu/F_A$, defined in eq 2, as obtained from the maximum values of the $\Delta G(t)$ transients for

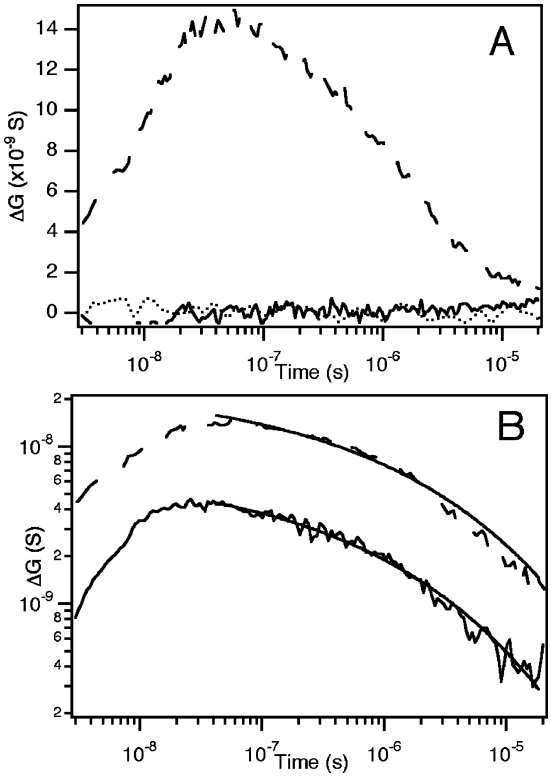


**Figure 2.** (A) Microwave conductance transients for a pure MDMO-PPV film (dotted), a ZnO film (full line), and the MDMO-$PPV_{0.67}$ blend film (dashed). (B) Microwave conductance transients for MDMO-$PPV_{0.67}$ (dashed) and $P3HT_{0.67}$ blend films (full line). The pure MDMO-PPV and ZnO films were excited at $\lambda = 510$ nm with an integrated intensity of $1 \times 10^{15}$ photons/cm$^2$ per pulse. The blend films were photoexcited at $\lambda = 510$ nm (MDMO-PPV) and $\lambda = 480$ nm (P3HT) with an intensity of $6 \times 10^{13}$ photons/cm$^2$ per pulse. The curves through the experimental data points in panel B are fits according to a stretched exponential. Note that both panels have a logarithmic *x*-axis, while the *y*-axis of panel A is linear and the *y*-axis of panel B is logarithmic.

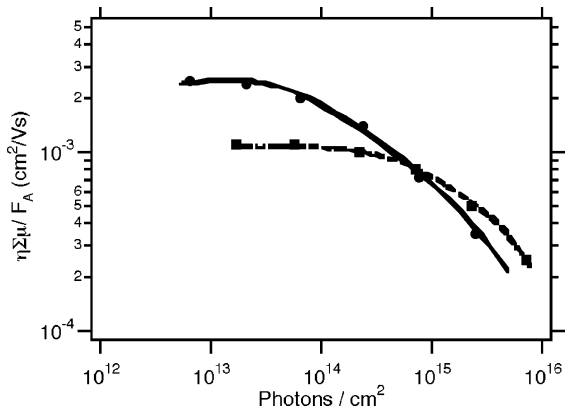


**Figure 3.** Photoconductivity per absorbed photon as function of intensity of photoexcitation for MDMO-$PPV_{0.67}$ (circles) and $P3HT_{0.67}$ (squares) blend films. The lines are guides to the eye. Note that $\eta\Sigma\mu/F_A$ becomes constant at low light intensities.

the blend films by photoexcitation with different laser pulse intensities. It can be seen that $\eta\Sigma\mu/F_A$ becomes intensity independent at intensities below $2 \times 10^{13}$ photons/cm$^2$ per pulse for MDMO-PPV and $2 \times 10^{14}$ photons/cm$^2$ per pulse for P3HT. Hence, below these threshold intensities, second-order processes such as exciton−exciton annihilation and bimolecular recombination of charge carriers do not play a significant role.[11,24]

The photoconductance transients in Figure 2 were recorded using a laser intensity of $6 \times 10^{13}$ photons/cm$^2$ per pulse. From

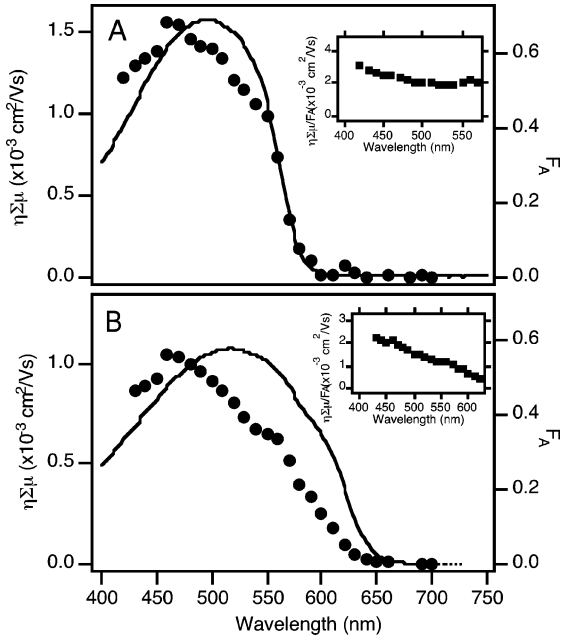


**Figure 4.** Action spectra (dots) and attenuation spectra (lines) of MDMO-$PPV_{0.67}$ (A) and $P3HT_{0.67}$ (B) blend films. The laser pulse intensity was ca. $10^{14}$ photons/cm$^2$ per pulse, depending on the wavelength. The inset shows the wavelength dependence of $\eta\Sigma\mu/F_A$.

Figure 3, it is clear that for this intensity the magnitude and decay of the photoconductance are mainly determined by (first-order) geminate recombination and/or trapping of the charge carriers (process G). It can be seen from Figure 2B that the magnitude of the photoconductance is higher for the MDMO-$PPV_{0.67}$ blend than for the $P3HT_{0.67}$ blend, while the decay kinetics is similar for these blends. The decay of the photoconductance can be described by a stretched exponential function ($\Delta G \sim \exp(-(t/\tau)^a)$), with $\tau = 0.6$ $\mu$s for MDMO-$PPV_{0.67}$, $\tau = 0.4$ $\mu$s for $P3HT_{0.67}$, and $a = 0.3$ for both blend films. A decay of the conductivity according to a stretched-exponential is characteristic for relaxation or decay of charge carriers undergoing dispersive transport in a disordered material, with the physical meaning of the parameter *a* depending on the relaxation mechanism.[25] A study of the origin of the stretched-exponential behavior for the present system is beyond the scope of this work.

**Photoconductance Action Spectra.** Action spectra for MDMO-$PPV_{0.67}$ and $P3HT_{0.67}$ blend films are shown in Figure 4A and B. The laser pulse intensity was slightly above the intensity-independence threshold. The action spectra are presented as $\eta\Sigma\mu$ instead of $\eta\Sigma\mu/F_A$, to facilitate comparison with the attenuation spectrum.

The onset of absorption at long wavelength coincides with that of the photoconductance for both blends. This corroborates the idea that the photoconductance results from excitation of the polymer (process A) and from subsequent exciton dissociation into free charge carriers at the interface with a cluster of ZnO nanoparticles (process D). For the MDMO-$PPV_{0.67}$ blend, the action and attenuation spectra are similar. In contrast, these spectra differ substantially for the $P3HT_{0.67}$ blend.

The values of $\eta\Sigma\mu/F_A$ in the insets in Figure 4A and B show that the quantum yield of charge carrier generation ($\eta/F_A$) increases as the wavelength is reduced, with the effect being most pronounced for the blend with P3HT. This could be due to the fact that the conformation of polymer chains in close vicinity to ZnO nanoparticles deviates more from planarity than chains in parts of the polymer film further away from ZnO. This would lead to a reduction of the effective conjugation

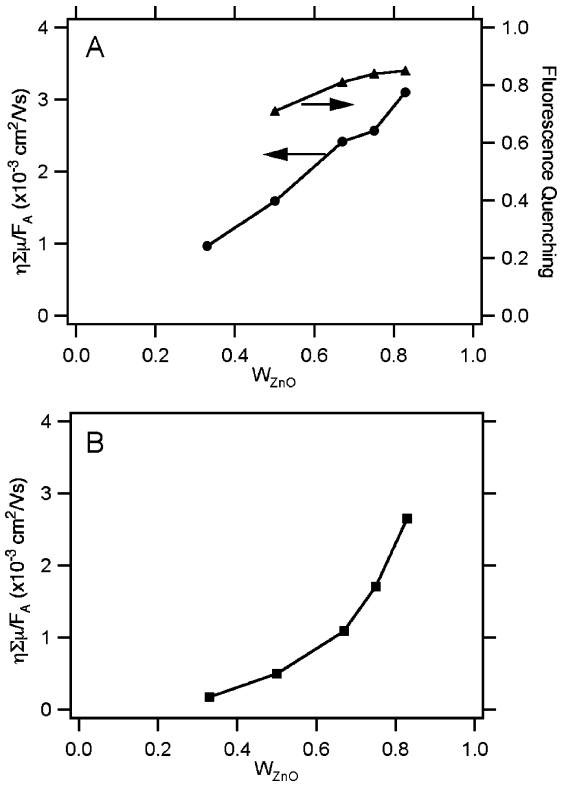


**Figure 5.** Conductivity per absorbed photon as a function of the weight fraction of ZnO in blend films with MDMO-PPV (A) or P3HT (B). The fluorescence quenching as measured by Beek et al.[15] is given on the right-hand axis in Figure 5A.

length and consequently a blue shift of the optical absorption by polymer chains near ZnO nanoparticles. Due to the limited diffusion length of excitons, the action spectrum resembles the blue-shifted attenuation spectrum of the disordered polymer near ZnO nanoparticles rather than that of the whole sample. An alternative explanation of the increase of $\eta/F_A$ with photon energy could be that the efficiency of dissociation of "hot" excitons or the exciton diffusion length increases with the photon energy.

**Influence of $W_{ZnO}$ on the Photoconductance.** Figure 5A and B show $\eta\Sigma\mu/F_A$ as a function of $W_{ZnO}$ in blends with MDMO-PPV and P3HT, respectively. For both blends, this parameter increases with $W_{ZnO}$. It must be noted that the photoconductance of different samples prepared from nominally identical batches of ZnO nanoparticles showed a similar dependence on $W_{ZnO}$; however, the absolute values of the photoconductance were found to vary by about a factor of 2. This variation of the photoconductance for samples that were prepared in an identical way is possibly due to differences in clustering of the ZnO nanoparticles.

Figure 5A also shows the fluorescence quenching as function of $W_{ZnO}$, which was measured in an earlier study by Beek et al.[15] It is interesting to note that the dependence of the fluorescence quenching on $W_{ZnO}$ is much less pronounced than the variation of $\eta\Sigma\mu/F_A$ with $W_{ZnO}$. This is most likely due to the fact that for low $W_{ZnO}$ quenching of excitons already occurs efficiently at the interface with individual ZnO nanoparticles (process C), while for higher $W_{ZnO}$ the amount of interfacial exciton (and fluorescence) quenching does not increase very much. However, the fraction of excitons that dissociates at the interface with a cluster of ZnO nanoparticles (process D) rather than at an individual nanoparticle (process C) will increase with $W_{ZnO}$. Consequently, $\eta\Sigma\mu/F_A$ depends more strongly on $W_{ZnO}$ than the fluorescence quenching.

The similar decay kinetics for the MDMO-PPV$_{0.67}$ and P3HT$_{0.67}$ blend films (see Figure 2B) suggests that the measured photoconductance in the blend of ZnO with MDMO-PPV is due to the same species as that in the blend with P3HT, i.e., excess electrons in ZnO. An estimate of the lower limit of the mobility of excess electrons in ZnO can be made as follows. For the samples studied, the highest value for $\eta\Sigma\mu/F_A$ is obtained for the MDMO-PPV$_{0.83}$ blend and amounts to $3 \times 10^{-3}$ cm$^2$/(V s) (see Figure 5A). Since $\eta/F_A \leq 1$, the lower limit to the electron mobility in ZnO is $3 \times 10^{-3}$ cm$^2$/(V s). This value is in agreement with mobilities reported earlier for interparticle hopping of electrons in nanoparticulate ZnO films.[26,27] The production of excess electrons in individual nanoparticles via process C is not expected to lead to a significant contribution to the photoconductance. From the observation that the onset of the absorption of ZnO nanoparticles varies with their size for a diameter near 5 nm,[21,22] it can be concluded that the excited electron is delocalized over the entire nanoparticle. Therefore, it is to be expected that an excess electron is also delocalized within the entire nanoparticle and moves with a diffusion constant which is close to that for bulk ZnO.[26,28] As a consequence of frequent electron scattering at the boundaries of the nanoparticle due to diffusive motion, the electron will not be able to move in phase with the 8.5 GHz oscillating microwave electric field and the intraparticle electron mobility as probed with the TRMC technique is negligible. Hence, in the present experiments, the observed photoconductance will be determined by the interparticle mobility of electrons, which is due to electron hopping from one ZnO nanoparticle to another within larger clusters of aggregated nanoparticles.

An increase of $W_{ZnO}$ leads to formation of larger clusters of ZnO nanoparticles.[15] As argued below, this does not result in an increase of the electron mobility as probed by the TRMC technique. For the amplitude of the electric field of the microwaves ($E = 100$ V/cm), the average net field induced drift displacement of electrons ($\delta r = \mu E \delta t$) during a half cycle of the microwave field ($\delta t = \sim 50$ ps) is only $\sim 0.5 \times 10^{-4}$ nm for an interparticle hopping mobility of the order of $10^{-3}$ cm$^2$/(V s), as reported in ref 26. This implies that the measured photoconductance is due to a slight microwave electric field induced bias in the otherwise diffusive motion of electrons along the direction of the field. Besides this, the root mean-square displacement due to diffusion ($r = \sqrt{(6Dt)}$ with $D = \mu kT/e$) during a cycle of the microwave field is only $\sim 1.3$ nm. Since the diffusive displacement and the net drift motion of the electrons during a cycle of the microwave field are very small compared to the center-to-center distance between nanoparticles in a cluster, the size of the clusters will not affect the interparticle hopping mobility as probed with the TRMC technique. Therefore, the observed increase of $\eta\Sigma\mu/F_A$ with $W_{ZnO}$ is not due to an increase in of the electron mobility with the size of the ZnO clusters.

The remaining possible origin of the experimentally observed increase of $\eta\Sigma\mu/F_A$ with $W_{ZnO}$ is an increase of the parameter $\eta/F_A$. On increasing $W_{ZnO}$, the fraction of excitons that dissociates at a larger ZnO cluster will become higher. The enhancement of exciton dissociation at the interface with a cluster of ZnO nanoparticles leads to the formation of a larger number of mobile electrons via process D. In addition, the yield of electrons that escape from geminate recombination and contribute to the photoconductance is expected to increase with the cluster size, analogously to what has been found earlier for a blend consisting of two polymers.[29] The larger amount of electrons injected in clusters of ZnO nanoparticles together with the larger yield of

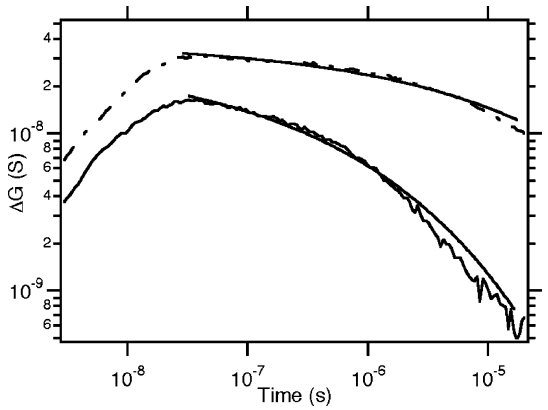


**Figure 6.** Microwave conductivity transients observed on photoexcitation at $\lambda = 480$ nm at an intensity of $2 \times 10^{14}$ photons/cm$^2$ per pulse of a P3HT$_{0.67}$ blend film before (full line) and after (dot−dash line) exposure of the sample to UV light (50 laser pulses at $\lambda = 300$ nm). The curves are fits of a stretched exponential function to the experimental data.

escape from geminate recombination (both effects lead to an increase of $\eta/F_A$) provide an explanation for the observed increase of $\eta\Sigma\mu/F_A$ with $W_{ZnO}$.

Comparison of Figure 5A and B shows that for low $W_{ZnO}$ the values of $\eta\Sigma\mu/F_A$ for ZnO:P3HT are smaller than for ZnO:MDMO-PPV blends. The value of $\eta\Sigma\mu/F_A$ for ZnO:P3HT blends increases more strongly with $W_{ZnO}$ than for ZnO:MDMO-PPV blends, and for $W_{ZnO} = 0.83$, the photoconductance of the two blends is almost equal. This can be explained in the following way. It has been found from atomic force microscopy (AFM) measurements[16] that the surface of blend films with P3HT is much rougher than that of blend films with MDMO-PPV, most likely due to formation of a smaller amount of much larger clusters of ZnO nanoparticles in P3HT. At low $W_{ZnO}$, the smaller amount of clusters will result in a smaller fraction of excitons quenching at a cluster of ZnO nanoparticles and consequently a lower value of $\eta\Sigma\mu/F_A$. In addition, the exciton diffusion length in P3HT[11] is shorter than that in MDMO-PPV,[3] and therefore, in blends with P3HT, less excitons will undergo interfacial charge separation at ZnO clusters. At higher $W_{ZnO}$, these effects will become less pronounced, because the average distance between clusters of ZnO nanoparticles is smaller, so that most excitons will quench at a cluster.

The data discussed above demonstrate that a relatively high value of $W_{ZnO}$ is needed for ZnO:P3HT blends in order to achieve a charge carrier yield, which is comparable to that for a corresponding ZnO:MDMO-PPV blend. In a solar cell, a high ZnO content is undesirable due to the loss of light absorption. The photovoltaic performance of ZnO:P3HT blends with a relatively low ZnO content can possibly be improved by formation of blend films in which the ZnO nanoparticles are more equally dispersed.

**Effect of UV Light.** Exposure of the blend films to visible light prior to the photoconductance measurements did not lead to any effect on the magnitude or the decay of the photoconductance. In addition, photoconductance transients measured for successive laser pulses at a repetition rate of 5 Hz were found to be similar. It is concluded from these observations that electrons and holes recombine within the time interval between successive laser pulses. In contrast, the data plots in Figure 6 show that exposure of the sample to UV light has a dramatic influence on the magnitude and the lifetime of the photoconductance of a ZnO:P3HT blend film. This figure shows TRMC signals of a P3HT$_{0.67}$ blend film prior to and after exposure to

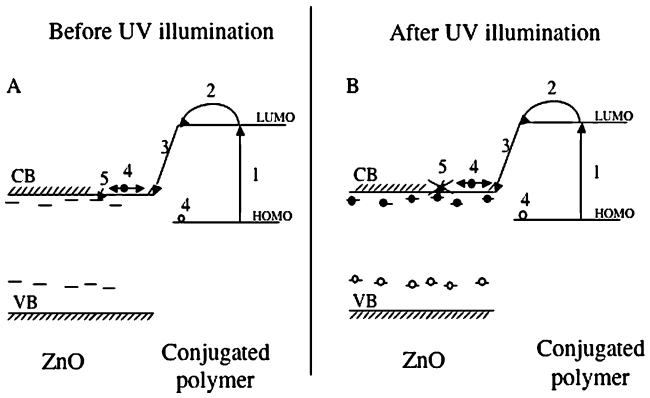


**Figure 7.** Schematic representation of energy levels and processes involved in the effects of UV illumination. Before UV illumination (A), excitation of the polymer with visible light (1), exciton diffusion (2), and electron injection (3) result in mobile electrons in ZnO, which contribute to the photoconductance (4) until the electron is trapped (5). After UV illumination (B), electron traps are occupied and electrons injected from the polymer are trapped to a lesser extent. As a result, the photoconductance becomes higher and decays on a longer time scale.

50 UV laser pulses ($\lambda = 300$ nm, $2 \times 10^{13}$ photons/cm$^2$ per pulse) at a repetition rate of 5 Hz. Before exposure to UV, a stretched-exponential fit ($\eta\Sigma\mu/F_A \sim \exp(-(t/\tau)^a)$) to the transient yields a decay time equal to 0.5 $\mu$s, which increases to 13 $\mu$s after UV exposure, while $a$ remains constant at 0.3. The decay time of the photoconductance of an MDMO-PPV$_{0.67}$ blend was also found to increase by exposure to UV.

An explanation for the effect of UV illumination is provided with the aid of Figure 7A and B, corresponding to the blend film before and after UV exposure, respectively. Exposure of the ZnO nanoparticles to UV light (Figure 7B) leads to direct excitation of electrons from the valence band to the conduction band. The positive charge carriers can populate deep hole traps within the band gap of ZnO nanoparticles, which have been attributed to the presence of oxygen vacancies.[20] According to Van Dijken et al.,[30,31] in the absence of oxygen at the surface of the ZnO nanoparticles (a condition which is fulfilled during our measurements), recombination of electrons with these deeply trapped holes occurs on a time scale ranging from minutes to hours.[30,32]

During this period, the electrons will also become trapped. Consequently, electrons that are subsequently injected from P3HT on photoexcitation in the visible (Figure 7B) encounter a reduced trap concentration on the ZnO nanoparticles as compared to the situation before UV illumination (Figure 7A), resulting in an increased magnitude and lifetime of the photoconductance. This explanation also corroborates the theory that the measured photoconductance is due to excess electrons in ZnO, as postulated above on basis of the similarity of the photoconductance transients for blends with MDMO-PPV and P3HT.

Illumination of a solar cell by UV light has been found to lead to a temporal disappearance of the photovoltaic effect.[18] On the basis of the discussion above, this can be understood as follows. UV illumination leads to the generation of electrons in ZnO, which fill the electron traps. After sufficient UV illumination, all electron traps are filled and subsequent illumination leads to the formation of free electrons. The presence of free electrons causes the ZnO to attain the properties of a conductor, and consequently, the photovoltaic behavior disappears.

## Conclusions

Blends of MDMO-PPV or P3HT as electron donors and (clusters of) ZnO nanoparticles as electron acceptors were studied by optical absorption spectroscopy and by time-resolved microwave conductivity measurements. The optical absorption spectra of MDMO-PPV blend films can be constructed from those of pure MDMO-PPV and of ZnO. In the spectrum of a pure P3HT film, a shoulder is observed at the long wavelength side of the absorption peak in the visible, which is attributed to aggregation of P3HT polymer chains. This shoulder vanishes gradually with an increasing weight fraction of ZnO, which is attributed to reduced aggregation of P3HT chains in the presence of ZnO.

Photoexcitation of the polymer in the blend films leads to a long-lived conductance signal, as a result of electron injection from the polymer into ZnO. From the finding that the kinetics of the decay of the photoconductance is similar for ZnO:MDMO-PPV and ZnO:P3HT blends and from the effects of UV illumination on the photoconductance, it is inferred that the measured photoconductance is due to excess electrons in ZnO.

For both the ZnO:MDMO-PPV and the ZnO:P3HT blend films, $\eta\Sigma\mu/F_A$ increases with the weight fraction ZnO. This increase is attributed to enhanced formation of mobile electrons resulting from interfacial exciton dissociation at clusters of ZnO nanoparticles rather than at individual nanoparticles. The dependence of the photoconductance on the weight fraction ZnO is found to be different for ZnO:MDMO-PPV and ZnO:P3HT blends. This is most likely due to the presence of a smaller number of relatively large ZnO clusters in ZnO:P3HT blends and a shorter exciton diffusion length, as compared with ZnO:MDMO-PPV blends.

Exposure of ZnO:P3HT blend films to UV light dramatically increases the magnitude and the lifetime of the photoconductance on excitation with visible light. This is attributed to filling of electron traps in ZnO during UV exposure. The metastable population of trapped electrons in ZnO reduces the trapping of electrons that are subsequently injected from P3HT on excitation in the visible. For blends with MDMO-PPV, a similar effect was observed.

**Acknowledgment.** The work of P.A.C.Q. (DPI 323) and M.M.W. (DPI 324) is part of the program Polymer Photovoltaics of the Dutch Polymer Institute. MDMO-PPV was provided by Philips Research Laboratories in Eindhoven, The Netherlands. The work of W.J.E.B. is supported by the Council for Chemical Sciences of the Netherlands Organization for Scientific Research (CW-NOW) in the Pionier program.

## References and Notes

(1) Brabec, C.; Dyakonov, V.; Parisi, J.; Sariciftci, N. S. *Organic Photovoltaics Concepts and Realization*; Springer: Heidelberg, 2003.
(2) O'Regan, B.; Gratzel, M. *Nature* **1991**, *353*, 737.
(3) Savenije, T. J.; Warman, J. M.; Goossens, A. *Chem. Phys. Lett.* **1998**, *287*, 148.
(4) Arango, A. C.; Johnson, L. R.; Bliznyuk, V. N.; Schlesinger, Z.; Carter, S. A.; Horhold, H. H. *Adv. Mater.* **2000**, *12*, 1689.
(5) van Hal, P. A.; Christiaans, M. P. T.; Wienk, M. M.; Kroon, J. M.; Janssen, R. A. J. *J. Phys. Chem. B* **1999**, *103*, 4352.
(6) Salafsky, J. S.; Lubberhuizen, W. H.; Schropp, R. E. I. *Chem. Phys. Lett.* **1998**, *290*, 297.
(7) Coakley, K. M.; McGehee, M. D. *Appl. Phys. Lett.* **2003**, *83*, 3380.
(8) Coakley, K. M.; McGehee, M. D. *Chem. Mater.* **2004**, *16*, 4533.
(9) Slooff, L. H.; Wienk, M. M.; Kroon, J. M. *Thin Solid Films* **2004**, *451*−*452*, 634.
(10) Ravirajan, P.; Haque, S. A.; Poplavskyy, D.; Durrant, J. R.; Bradley, D. D. C.; Nelson, J. *Thin Solid Films* **2004**, *451*−*452*, 624.
(11) Kroeze, J. E.; Savenije, T. J.; Vermeulen, M. J. W.; Warman, J. M. *J. Phys. Chem. B* **2003**, *107*, 7696.
(12) Huisman, C. L.; Goossens, A.; Schoonman, J. *Chem. Mater.* **2003**, *15*, 4617.
(13) Coakley, K. M.; Liu, Y. X.; McGehee, M. D.; Frindell, K. L.; Stucky, G. D. *Adv. Funct. Mater.* **2003**, *13*, 301.
(14) Beek, W. J. E.; Wienk, M. M.; Janssen, R. A. J. *Adv. Mater.* **2004**, *16*, 1009.
(15) Beek, W. J. E.; Wienk, M. M.; Kemerink, M.; Yang, X.; Janssen, R. A. J. *J. Phys. Chem. B* **2005**, *109*, 9505.
(16) Beek, W. J. E.; Wienk, M. M.; Janssen, R. A. J. *Adv. Funct. Mater.* **2005**, in press.
(17) Martens, H. C. F.; Blom, P. W. M.; Schoo, H. F. M. *Phys. Rev. B* **2000**, *61*, 7489.
(18) Beek, W. J. E. Hybrid Polymer Solar Cells. Ph.D. Thesis, Eindhoven University of Technology, Eindhoven, The Netherlands, 2004.
(19) Wegewijs, B. R.; Dicker, G.; Piris, J.; Garcia, A. A.; de Haas, M. P.; Warman, J. M. *Chem. Phys. Lett.* **2000**, *332*, 79.
(20) van Dijken, A.; Meulenkamp, E. A.; Vanmaekelbergh, D.; Meijerink, A. *J. Lumin.* **2000**, *90*, 123.
(21) Pesika, N. S.; Stebe, K. J.; Searson, P. C. *J. Phys. Chem. B* **2003**, *107*, 10412.
(22) Pesika, N. S.; Stebe, K. J.; Searson, P. C. *Adv. Mater.* **2003**, *15*, 1289.
(23) Brown, P. J.; Thomas, D. S.; Kohler, A.; Wilson, J. S.; Kim, J. S.; Ramsdale, C. M.; Sirringhaus, H.; Friend, R. H. *Phys. Rev. B* **2003**, *67*, 064203-1−064203-16.
(24) Savenije, T. J.; Kroeze, J. E.; Wienk, M. M.; Kroon, J. M.; Warman, J. M. *Phys. Rev. B* **2004**, *69*, 155205-1−155205-11.
(25) Dicker, G.; de Haas, M. P.; de Leeuw, D. M.; Siebbeles, L. D. A. *Chem. Phys. Lett.* **2005**, *402*, 370.
(26) Meulenkamp, E. A. *J. Phys. Chem. B* **1999**, *103*, 7831.
(27) Noack, V.; Weller, H.; Eychmuller, A. *J. Phys. Chem. B* **2002**, *106*, 8514.
(28) Enright, B.; Fitzmaurice, D. *J. Phys. Chem.* **1996**, *100*, 1027.
(29) Quist, P. A. C.; Savenije, T. J.; Koetse, M. M.; Veenstra, S. C.; Kroon, J. M.; Siebbeles, L. D. A. *Adv. Funct. Mater.* **2005**, *15*, 469.
(30) van Dijken, A.; Meulenkamp, E. A.; Vanmaekelbergh, D.; Meijerink, A. *J. Phys. Chem. B* **2000**, *104*, 4355.
(31) van Dijken, A.; Meulenkamp, E. A.; Vanmaekelbergh, D.; Meijerink, A. *J. Phys. Chem. B* **2000**, *104*, 1715.
(32) Shim, M.; Guyot-Sionnest, P. *J. Am. Chem. Soc.* **2001**, *123*, 11651.